Journal of Medicinal Chemistry Article

J. Med. Chem. **2010,** *53,* 6457–6465 **6457**
DOI: 10.1021/jm1007853

Interaction of Daunomycin with Acetylated Chromatin

Lyndsay Sprigg,[†] Andra Li,[†] Francis Y. M. Choy,[‡,§] and Juan Ausió*[,†,§]

[†]*Department of Biochemistry and Microbiology, University of Victoria, Victoria, British Columbia, V8W 3P6, Canada,* [‡]*Department of Biology, University of Victoria, Victoria, British Columbia, V8W 3P6, Canada, and* [§]*Center for Biomedical Research, University of Victoria, Victoria, British Columbia, V8W 3N5, Canada*

Received June 29, 2010

Anthracyclines are powerful chemotherapeutic agents for the treatment of many cancers. In many instances, they are currently used in combination with histone deacetylase inhibitors in order to enhance their efficiency. Not surprisingly and as part of their mode of action, these drugs interfere with gene expression, a process that has long been known to be mediated by histone acetylation. In this paper, we use analytical ultracentrifuge analysis, equilibrium dialysis, and circular dichroism to characterize the role of histone acetylation on the binding of antharcyclines to chromatin. We show that histone acetylation enhances the daunomycin-induced DNA dissociation from nucleosomes and decreases the extent of aggregation that results from the interaction in a way that is modulated by the presence or absence of linker histones. Histone acetylation increases the binding affinity of daunomycin by chromatin. Furthermore, the binding of anthracycline to acetylated chromatin sheds additional light into the conformational chromatin alterations resulting from core histone acetylation.

Introduction

Anthracycline antibiotics have been studied extensively since their isolation from *Streptomyces* sp. in the early 1950s. Their extensive antibiotic activity has made these compounds the subject of considerable interest. However, the observed toxicity of these drugs slowed the development of anthracyclines as therapeutic agents. It was not until the discovery of daunomycin in the early 1960s that anthracyline antibiotics began to advance as antineoplastic agents.[1,2] Although daunomycin has been routinely used in the treatment of myelogenous leukemia,[3,4] today it is being used in combination with other chemotherapeutic agents to treat a broad variety of different types of cancer. For instance, in combination with tamoxyfen, daunomycin is currently used for the treatment of breast cancer.[5]

Daunomycin ($C_{27}H_{29}NO_{10}$) consists of planar tetracycline rings linked to a pyranose sugar moiety (see Figure 1). Evidence has shown that these drugs act on nuclear DNA, the genetic material of cells.[6−8] The planar structure facilitates intercalation of the drug between base pairs.[9,10] The anthraquinone chromophore inserts perpendicularly into the long dimension of the adjacent DNA base pairs. The tetrahydropyran ring sits in the minor groove of DNA where the substituents undergo hydrogen bond interactions with the bases above and below the site of insertion stabilizing the complex. The amino sugar also rests in the minor groove with the positive charge possibly adding an electrostatic interaction. The stereoisomeric configuration of the sugar on daunomycin greatly affected and diminished the affinity of the drug for DNA when altered, implying that the drug−DNA interaction is stereospecific.[11,12]

Although the daunomycin studies utilizing DNA template have produced valuable insight into possible intracellular mechanisms of anthracycline antibiotics, it is important to consider the effects of proteins and the nuclear environment within living cells. DNA within the eukaryotic cell exists with an array of associated proteins responsible for the ordering and assembly of DNA in a complex known as chromatin. Although the conclusions that can be drawn from studies conducted with DNA are valuable in deducing potential mechanisms of action of anthracyclines, the target within living cells would be chromatin and not free DNA.[12,13] Associations between the DNA and protein in chromatin may alter the interactions observed of anthracyclines and free DNA and possibly lead to variation in the observed activity of the intercalators. As chromatin is the primary target within eukaryotic cells, it is essential that the anthracycline interactions also be studied with chromatin template.

Early studies in chromatin−anthracyline interactions revealed a reduced affinity for nucleosomes in comparison to free DNA.[13,14] DNA synthesis was shown to be stunted by the intercalation of anthracyclines with inhibition dependent upon the strength of the association with DNA or nucleosome.[13] It was postulated that the preference for free DNA likely involves the geometry of the DNA−daunomycin interaction. Anthracycline antibiotics appear to protrude on either side of the DNA helix after intercalation. These protrusions on either side of the helix may explain the preference of anthracyclines for free DNA over bent DNA such as that found in nucleosomes.[10,15,16] Generally, studies are in agreement that the affinity of anthracyclines is greatest for free

*To whom correspondence should be addressed. Address: Department of Biochemistry and Microbiology, University of Victoria, P.O. Box 3055, Petch Building, 220, Victoria, British Columbis, V8W 3P6, Canada. Phone: 250-721 8863. Fax: 250-721 8855. E-mail: jausio@uvic.ca.

Published on Web 08/10/2010

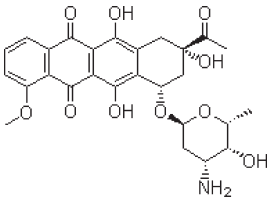

Figure 1. Structure of daunomycin structure including a tetracycline ring linked through a glycosidic bond to a single amino sugar.[9]

DNA, followed by affinity for the 175 base pair (bp[a]) nucleosome which contains the core particle as well as linker DNA, with the least affinity for nucleosome core particle.[16] However, contradicting evidence still remains about cooperativity of binding; results appear to vary between techniques used and require further investigation.[13,15,17]

The presence of histone H1 has been shown to reduce the interaction of daunomycin even further than that observed with the core histones.[12,13,17] This observation is consistent with the concept that daunomycin preferentially interacts with free DNA. When H1 occupies the linker region, further folding the chromatin fiber, the geometry of the DNA is altered and sites available for stereospecific intercalation are reduced.[10,15,16]

A further layer to consider when studying chromatin interactions is posttranslational modifications. Posttranslational modifications such as acetylation are essential for DNA metabolism and can affect the conformation of chromatin. Global histone acetylation primarily occurs at the basic region of N-terminal histone tails on lysine, and the ensuing neutralization of the positive charge at the affected residues is thought to weaken their interaction with negatively charged DNA.[18] As a result, the nucleosome adopts an altered,[19−21] less stable conformation[22] and the chromatin fiber becomes more relaxed,[23] particularly in histone H1-defficient chromatin.[24,25]

Although the mode of action of daunomycin is still not very clear and it may have multifaceted effects,[12] it has been shown to interfere with RNA synthesis[26] as recently exemplified by its role in the transcriptional regulation of neural sphingomyelinase 2 gene expression.[27] Therefore, as histone acetylation has long been associated with transcriptionally active DNA,[28−30] we reasoned that it would be important to characterize the role of histone acetylation in the modulation of the interaction of daunomycin with chromatin.

In this paper, we have investigated differential interactions of daunomycin with acetylated mononucleosomes and long chromatin obtained from chicken erythroleukemic cells and compared these findings with previously described interactions with native counterpoints. These results were also compared to the same chromatin fractions upon depletion of linker histone. The interactions were characterized by sedimentation velocity analytical ultracentrifuge (AUC) analysis, circular dichroism (CD), and equilibrium dialysis.

[a] Abbreviations: bp, base pair; AUC, analytical ultracentrifuge; CD, circular dichroism; MSB, chicken erythroleukemic cells transformed by Marek's virus; DMEM, Dulbecco's modified Eagle's medium; TLC, thin layer chromatography; HPLC, high performance liquid chromatography; SDS, sodium dodecyl sulfate; PIPES, piperazine-*N*,*N*′-bis(2-ethanesulfonic acid) buffer; EGTA, ethylene glycol tetraacetic acid; EDTA, ethylenediaminetetraacetic acid; A_{260}, absorbance at 260 nm; Tris, tris(hydroxymethyl)aminomethane; PAGE, polyacrylamide gel electrophoresis; AU, acetic acid−urea; c_f, concentration of free daunomycin in dialysate; *r*, the ratio of bound drug to total base pair concentration; *K*, the apparent binding constant; rpm, rotations per minute; SE, supernatant containing chromatin.

Experimental Procedures

Materials. Chicken erythroleukemic cells transformed by Marek's virus (MSB) were grown in the absence (native) and presence (acetylated) of 5 mM sodium butyrate as previously described.[31] Cells were stored in Dulbecco's modified Eagle's medium (DMEM) containing 40% glycerol at −80 °C until thawed for chromatin preparation as described below. Micrococcal nuclease was obtained from Worthington Biochemicals. Daunomycin hydrochloride was obtained from Sigma-Aldrich, and ≥95% purity was confirmed by thin layer chromatography (TLC) and high performance liquid chromatography (HPLC). Stock solutions of daunomycin were prepared using sterile distilled water to 5 mg/mL and aliquoted in small volumes. The stock solutions were stored in the dark at −20 °C until use. Further dilutions of the drug were prepared in the desired buffer immediately prior to experimental procedures.

Preparation of Mononucleosomes. MSB cell nuclei were obtained for native and acetylated samples as described previously.[31] The concentration of DNA in the nuclear suspension was determined in the presence of 0.5% sodium dodecyl sulfate (SDS) using an extinction coefficient absorbance at 260 nm (A_{260}) of 20 $cm^2\ mg^{-1}$. The nuclear suspension at A_{260} = 80 $cm^2\ mg^{-1}$ in 50 mM NaCl, 10 mm piperazine-*N*,*N*′-bis(2-ethanesulfonic acid) buffer (PIPES pH 6.8), 5 mM $MgCl_2$, 1 mM $CaCl_2$ (with or without 10 mmM sodium butyrate) was digested with 120 units of micrococcal nuclease/mL at 37 °C for 10 min with gentle shaking. After digestion the solution was brought to 5 mM ethylene glycol tetraacetic acid (EGTA) on ice and immediately centrifuged at 9800*g* for 5 min at 4 °C. The pellet was resuspended in 0.25 mM ethylenediaminetetraacetic acid (EDTA pH7.5) and gently stirred at 4 °C for 1 h to lyse nuclei. The lysate was centrifuged at 12100*g* for 17 min at 4 °C. The supernatant containing chromatin (SE) was collected, one-half to remain with linker histone (+H1) and the other to be stripped (−H1) of linker histone (see Preparation of H1-Depleted Mononuclesomes). All four chromatin samples obtained (native +H1 and −H1 and acetylated +H1 and −H1) were loaded on a 5−20% sucrose gradient in 25 mM NaCl, 10 mM tris(hydroxymethyl)aminomethane (Tris)-HCl (pH 7.5), 0.25 mM EDTA and centrifuged at 93350*g* for 21 h at 4 °C. Fractions along the gradient were collected at 1 mL/min, and absorbance at A_{260} was determined (Cary UV−visible spectrophotomer). DNA size of the different fractions was analyzed using native polyacrylamide gel electrophoresis (PAGE), and their histone composition was visualized using either SDS−PAGE or acetic acid−urea (AU)−PAGE (see below). Fractions of interest were combined and dialyzed in 10 mM Tris-HCl (pH 7.5), 5 mM NaCl, 0.5 mM EDTA. "Complete" protease inhibitor (Roche Moleculare Biochemicals) was added (1 tablet per 100 mL), and samples were stored on ice until further use.

Preparation of Long Chromatin. Nuclear suspensions were obtained as described above. The nuclear suspension at A_{260} = 120 was digested with 8 units of micorcoccal nuclease/mL of suspension at 37 °C for 5 min with gentle shaking. The preparation was continued as described above. Obtained SE chromatin samples were fractionated using centrifugation with 5−20% (w/v) sucrose gradient in 25 mM NaCl, 10 mM Tris-HCl (pH 7.5), 0.25 mM EDTA and centrifuged at 93350*g* for 3 h at 4 °C. Fractions along the gradient were collected at 1 mL/min, and absorbance at A_{260} was determined (Cary UV−visible spectrophotomer). State of chromatin folding was analyzed using the analytical ultracentrifuge and comparing sedimentation for chromatin samples in low salt [5 mM NaCl, 10 mM Tris-HCl (pH 7.5), 0.5 mM EDTA] and high salt [80 mM NaCl, 10 mM Tris-HCl (pH 7.5), 0.5 mM EDTA] buffers. Histone composition was examined using SDS−PAGE/AU−PAGE.

Preparation of H1-Depleted Mononuclesomes. Prior to sucrose gradient fractionation of chromatin, the samples to be stripped of H1 were brought to a final NaCl concentration of

0.35 M by quick addition of 5 M NaCl while vortexing. Samples were tumbled with CM Sephadex C-25 Sephadex resin at a ratio of 12 mg of resin/mg of DNA for 1.5 h at 4 °C.[32] The resin had been previously equilibrated in 0.35 M NaCl, 10 mM Tris-HCl, pH 7.5, and 0.25 mM EDTA. The resin suspension was next centrifuged at 3500*g* for 10 min at 4 °C, and then supernatant consisting of H1-depleted chromatin was collected and fractionated by centrifugation using a 5−20% sucrose gradient as described above.

Preparation of H1-Depleted Long Chromatin. Histone H1 removal was conducted as previously described.[17] Briefly, chromatin fractions of interest were obtained as described above and dialyzed overnight against 50 mM NaCl, 10 mM Tris-HCl (pH 7.5), 0.1 mM EDTA at 4 °C. Samples were concentrated with Centriprep 50 concentrator (Amicon Ltd.) and loaded onto a CM Sephadex C-25 (1 cm × 12 cm) column that had been preequilibrated with the same buffer overnight. The column was eluted at a flow rate of 6 mL/h at 4 °C. Fraction absorbance at A_{260} was determined, and fractions of the chromatin peak were pooled and dialyzed in 10 mM Tris-HCl (pH 7.5), 5 mM NaCl, 0.1 mM EDTA. The dialysate was treated with "Complete" protein inhibitor and stored on ice for future use, as described above.

Gel Electrophoresis. SDS−PAGE was carried out according to Laemmli.[33] AU−PAGE was carried out as described elsewhere.[19] In this later case the chromatin samples to be analyzed were dissolved in 4 M urea, 5% acetic acid, and 0.5% (w/v) protamine sulfate (to displace the histones from DNA) and incubated at 65 °C for 15 min before loading them onto the gel.[34] Native 4% PAGE for DNA analysis was preformed as previously described by Yager and van Holde.[35]

Equilibrium Dialysis. Acetylated chromatin in the absence and presence of H1 at 40−45ug/mL in 10 mM Tris, 5 mM NaCl, and 0.1 mM EDTA was dialyzed against the same buffer with increasing concentrations of daunomycin as previously described.[17] Dialysis was carried out at 4 °C using Spectra/Por 2 (Spectrum companies). Equilibrium was established for 72 h with no detectable binding of drug to the membrane. Concentration of free daunomycin in dialysate (c_f) was measured by absorbance at 480 nm. The Scatchard method was used to determine binding parameters from r/c_f versus r plot where r is the ratio of bound drug to total base pair concentration.[36] K, the apparent binding constant, is the negative value of the slope of the curve.

Analytical Ultracentrifuge Analysis. Chromatin fractions were dialyzed against 5 mM NaCl, 10 mM Tris-HCl (pH7.5), 0.1 mM EDTA overnight at 4 °C. Mononuclesome samples (30−35 μg/mL) were incubated with the appropriate daunomycin ratios of 0, 0.167, 0.334, 0.669, and 1.34 mol daunomycin/mol bp of DNA (0, 5, 10, 20, or 40 μg/mL) for 10 min at 20 °C. Long chromatin samples were incubated with daunomycin ratios of 0, 0.167, 0.334, 0.501, 0.669, 0.835, and 1.34 mol daunomycin/mol bp of DNA (0, 5, 10, 15, 20, 25, or 40 μg/mL) for 10 min at 20 °C. Nucleosomes concentration was adjusted to 30−35 μg/mL using dialysis buffer. The molar amount of daunomycin was determined for each desired concentration used using a molecular weight of 563.9. AUC analysis was carried out on a Beckman XL-A ultracentrifuge using an An-55 aluminum rotor and double sector aluminum-filled Epon centerpieces. Runs with mononucleosomes were conducted at 20 °C, 40 000 rotations per minute (rpm). Runs with long chromatin were conducted at 20 °C, 17000 rpm. Plots were generated using Ultrascan 5.0 software using van Holde−Weischet analysis and second moment of velocity data.[37] To evaluate the folding potential of chromatin samples, each sample was examined in low salt (10 mM Tris-HCl (pH 7.5), 5 mM NaCl, 0.1 mM EDTA) and high salt (10 mM Tris-HCl (pH 7.5), 80 mM NaCl, 0.1 mM EDTA). Each sample was dialyzed overnight in the corresponding buffer, and sedimentation analysis was conducted at 20 °C, 17 000 rpm, 11 scans per cell.

Circular Dichroism Spectroscopy. CD spectroscopy experiments were conducted on a Jasco-J720 spectropolarimeter in a 1 cm path length cuvette. The CD spectra were recorded between 350−450 nm and 210−300 nm at a scan rate of 200 nm/min, bandwidth 1 nm, average speed 0.125 s, accumulation of 4 scans. Samples used for CD analysis were identical to those used in sedimentation analysis of long chromatin. The same molar ratios of daunomycin were used to conduct these experiments. Chromatin fractions were dialyzed against 5 mM NaCl, 10 mM Tris-HCl (pH 7.5), 0.1 mM EDTA overnight. Chromatin samples were incubated with the appropriate daunomycin ratios of 0, 0.167, 0.334, 0.669, and 0.835 mol daunomycin/mol bp of DNA for 10 min at 20 °C prior to loading into the CD cuvette. The computer directly interfaced to the spectropolarimeter performed data analysis.

Results and Discussion

Cooperative binding of daunomycin to nucleosomes induces DNA dissociation and nucleosome aggregation in a way that depends on the extent of acetylation and the presence of linker histones. In order to characterize the interaction of daunomycin with nucleosomes consisting of acetylated histones,[19] nuclei from erythroleukemic MSB cells grown in the presence of histone deacetylase inhibitor sodium butyrate[23] were digested with micrococcal nuclease and the chromatin fragments released were subsequently fractionated by sucrose gradients. Nucleosomes lacking histone H1 were obtained by mild linker histone depletion from nuclease digested chromatin previously to sucrose gradient fractionation. Figure 2 shows the biochemical characterization of the nucleosome particles thus obtained. The average extent of histone acetylation estimated from the AU−PAGE analysis (bottom part, right-hand side of Figure 2) was determined to be 10−12 acetyl groups per nucleosome.[19]

Histone acetylation alters the structure of the nucleosome which adopts a more extended conformation[19] in a way that has been interpreted to be the result of a partial release of the flanking DNA ends at the entry and exit sites.[24,25] Conversely, this has also been suggested to be due to a distortion of the nucleoprotein particle itself.[20] Regardless of the molecular mechanism involved, such structural alterations arise from a weakening of the histone−DNA interactions resulting from the neutralization of the charge at the ε-amino groups of the acetylated lysines which decrease stability of the particle.[22] Such structural changes have the potential to increase DNA accessibility to DNA counterions and DNA binding drugs.

The results shown in Table 1 are in agreement with the notion of the nucleosome particle adopting a more relaxed conformation as the net charge in the DNA increases or as the neutralization of this charge by the histone tails/linker histones decreases. Indeed, a gradual but noticeable decrease in the sedimentation coefficient of the particle is observed in the progression from native nucleosomes to linker-depleted nucleosomes, all of which is enhanced by core histone acetylation in agreement with previously published results.[19]

Figure 3A shows the sedimentation behavior of native nucleosomes lacking histone H1 in the absence of daunomycin in comparison to the same nucleosomes in the presence of 0.167 mol of drug per mole of DNA. While the sedimentation of the former exhibits a monodisperse distribution, the latter shows a much more complex situation. In this instance the unperturbed 12 S nucleosome component coexists with a heterogeneous mixture consisting of fully dissociated (5 S) and a 9 S component in addition to aggregated complexes with higher sedimentation coefficients (15−24 S). The same behavior is observed in the case of the acetylation sample

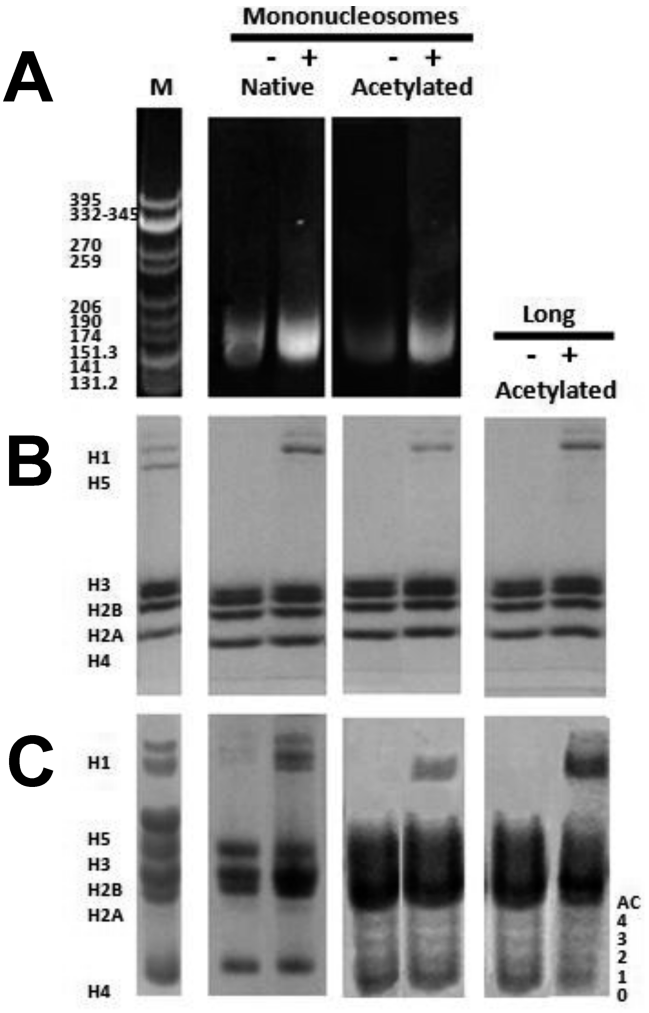

Figure 2. Compositional characterization of the mononucleosomes and chromatin fractions used in this work. (A) Native PAGE of the DNA extracted from native and acetylated nucleosome samples containing (+) or lacking (−) histone H1. M is a *Cfo*I-cut pBR322 marker. (B) SDS−PAGE of mononucleosomes and chromatin fractions. (C) AU−PAGE analysis of mononucleosomes and chromatin fractions. The numbers on the right-hand side of this panel refer to the number of acetyl groups present in histone H4.

Table 1. Sedimentation Coefficient ($s_{20,w}$) of Native and Acetylated Mononucleosomes Containing (+H1) or Lacking (−H1) Histone H1 in 5 mM NaCl, 10 mM Tris-HCl (pH 7.5), 0.1 mM EDTA

nucleosome sample	$s_{20,w}$
native, +H1	12.4 S
native, −H1	12.2 S
acetylated, +H1	12.0 S
acetylated, −H1	11.6 S

(not shown). In the presence of H1, the pattern lacks resolution and only a broad peak corresponding to the intact nucleosome and a 23 S peak corresponding to aggregates are seen for the acetylated and unacetylated samples. The lack of resolution in this instance is probably due to the presence of H1 which increases the complexity of the sedimentation pattern beyond the resolution of the method used here for the analysis. The presence of a 9 S peak in the absence of histone H1 had been previously observed (9.45 S) in native nucleosomes lacking H1 at daunomycin (mol bp ratios of ≤0.15) and has been attributed to nucleosome unfolding.[16] This sedimentation coefficient corresponds to that of nucleosomes lacking a histone H2A−H2B dimer[38] (but see below) and could also correspond to a nucleosome with an extended conformation in which the flanking ends of the DNA are stretched as a result of the binding of the drug in these regions. Indeed the binding of daunomycin is highly cooperative[17] and it has a strong preference for the linker DNA[16] (see also the long chromatin section). The preferential binding of daunomycin to the linker DNA regions not constrained by the interactions with the core histones is not surprising. In addition to the potential site occlusion imposed by the histone binding, the core histone−DNA interactions result in a nucleosomally constrained DNA with a highly distorted B-conformation[39] that may further hinder the intercalation of daunomycin between adjacent base pairs. Hence, the binding of daunomycin to nucleosomes is likely to start at the ends of the DNA flanking the particle and proceed inward toward the middle resulting in a loss of stability that subsequently leads to aggregation. Consistent with this notion, at ratios higher than 0.167 mol drug/mol bp, the complexity of the sedimentation pattern increases (see Figure 3B) with that of nucleosomes containing histone H1 exhibiting a more complex pattern. At a higher ratio corresponding to 0.669 mol drug/mol bp most of the sample behaves as free 5 S DNA, especially in the acetylated counterparts (Figure 3C).

The length of the DNA in the nucleosomes used in this work was 165 ± 5 bp (Figure 2). Considering that daunomycin is an intercalator[40] and that the binding is cooperative[17] as discussed earlier, this means that saturation of binding should occur at 0.5 mol drug/mol bp. As can be seen in Figure 4A, the transition toward aggregation takes place at approximately 0.15 mol drug/mol bp[16] irrespective of whether the nucleosome is acetylated or not (Figure 4A). Under cooperative binding, approximately 30% of the DNA is interacting with the drug at this ratio which corresponds to approximately 50 bp being bound by the drug. A cooperative binding model with the intercalation of daunomycin proceeding from both ends of the DNA in the nucleosome particle would result in only 115 bp of DNA bound to the histone octamer. A situation like this could lead to histone H2A−H2B dissociation and/or directly result in nucleosome aggregation such as is observed in nucleosomes that have been overdigested by nucleases below the 125−120 bp range.[41] A nucleosome lacking an H2A−H2B dimer has been visualized by native PAGE during binding of ethidium bromide to nucleosomes.[42] However, we could not detect any such subnucleosome particle at any of the mol daunomycin/mol bp used by us when using the same electrophoretic system (Figure 4B). Instead, a small but noticeable retardation in the electrophoretic migration of the band corresponding to the nucleosome is observed (see upper arrowhead in Figure 4B) that likely corresponds to an extended conformation of the particle. Regardless of the nucleosome conformational transition, the DNA dissociation involved depends on breaking the interactions of the histone fold with the DNA needed to maintain the nucleosome stability. The size and complexity of the aggregates ensuing this dissociation are dependent on histone H1 and on the extent of acetylation of the core histone tails (see Figure 3B−C and Figure 4A).

Histone acetylation increases the affinity of daunomycin by chromatin. The binding constants of daunomycin by acetylated chromatin determined as described previously[17] (Figure 5A and Table 2) indicate a higher affinity of daunomycin by

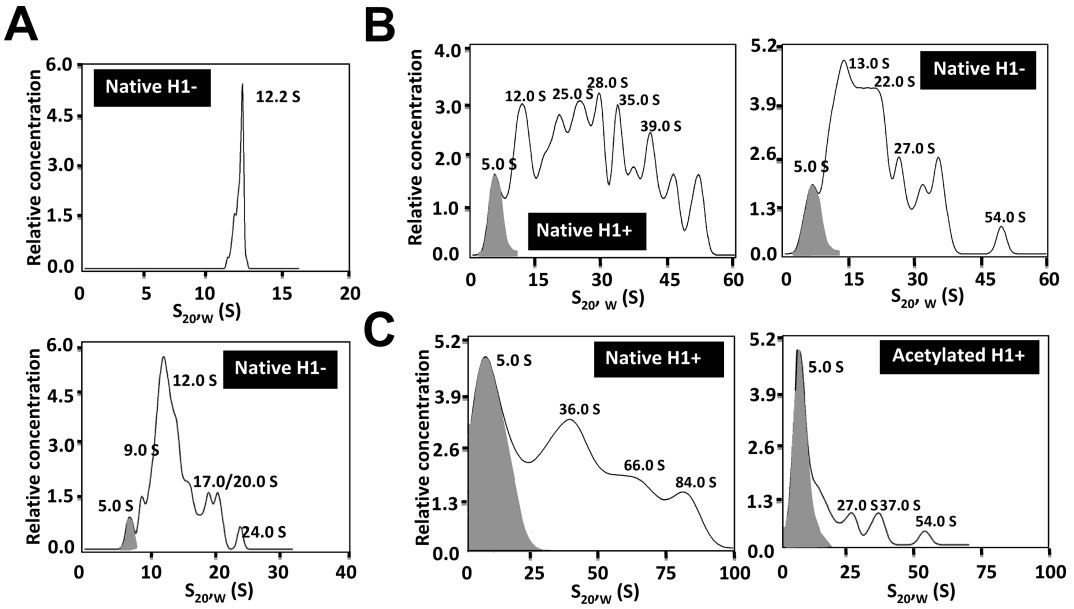

Figure 3. Sedimentation velocity analyses of native and acetylated nucleosomes containing (H1+) or lacking (H1−) histone H1at different concentrations of daunomycin. (A) Upper panel, 0.000 mol daunomycin/mol bp; lower panel, 0.167 mol daunomycin:mol bp. (B) 0.334 mol daunomycin/mol bp. (C) 0.669 mol daunomycin/mol bp. The plots shown correspond to the relative sample concentration as a function of the sedimentation coefficient using the histogram envelope analysis from the UltraScan software (see Experimental Procedures). The $s_{20,w}$ values of the main peaks are shown. The shaded area corresponds to the fraction of dissociated nucleosomes sedimenting as free (5 S) DNA.

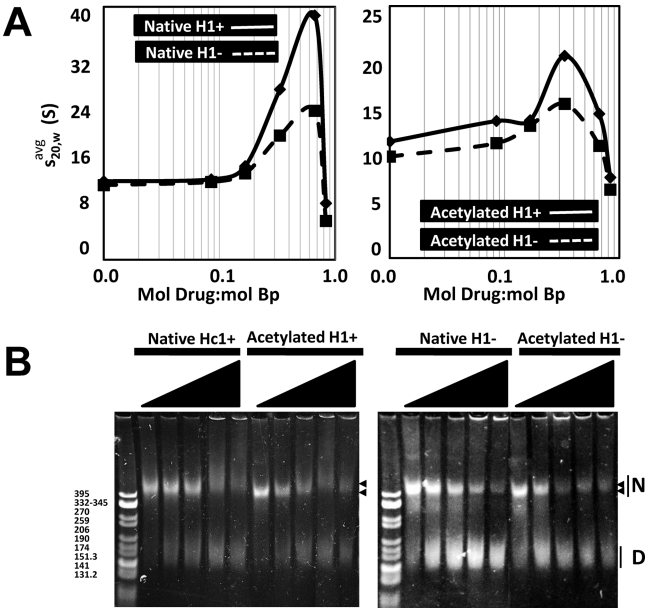

Figure 4. Electrophoretic and sedimentation velocity analyses of native and acetylated nucleosomes as a function of the mol daunomycin/mol bp. (A) Dependence of the average sedimentation coefficient $s_{20,w}{}^{avg}$ (determined from the second moment analysis as indicated in Experimental Procedures) as a function of mol daunomycin/mol bp. (B) Native (4%) PAGE analysis of mononucleosome fractions incubated with 0, 0.167, 0.669, 1.34, and 2.68 mol daunomycin/mole bp of DNA. N: nucleosome. D: free DNA (dissociated nucleosome DNA). Notice that the amount of free DNA appears constant throughout the titration even at the higher mol drug/mol bp ratios where in the centrifuge most of the material is free 5 S DNA (Figure 3B). This is most likely due to the inability of ethidium bromide (which is used to stain the DNA) to efficiently displace the bound daunomycin. The two arrowheads indicate the change in the band corresponding to the nucleosome mobility as the ratio (mol daunomycin/mol bp of DNA) increases.

acetylated chromatin irrespective of the presence or absence of histone H1. The hydrodynamic analysis (Figure 5B) is consistent with results published earlier with equivalent native chromatin fractions.[17] Globally, these data support the notion that the affinity of daunomycin for chromatin increases with the number of base pairs in the regions of DNA flanking the DNA coils directly bound by the core of the histone octamer.[17]

The sedimentation velocity analysis carried out in this work was performed on an acetylated chromatin fraction before or after depletion of its associated linker histones (histone H1). Previous to any drug interaction studies the two samples were characterized for their ability to properly fold upon increasing the ionic strength of the media (Table 3). The characterization of the NaCl dependence of chromatin folding for both native[43] and acetylated chromatin fractions in the absence or presence of histone H1 has been well documented in the past.[23,25] The shift observed in the concentration of daunomycin required to decrease the sedimentation coefficient ahead of aggregation (Figure 5B) is in agreement with a more extended lower association of the DNA flanking regions with the nucleosome when histones are acetylated.[19,24] The minimum $s_{20,w}$ value corresponding to this decrease shifts from approximately 0.33 in the native chromatin to 0.5 for the acetylated chromatin fraction containing histone H1. In the fractions depleted of histone H1 the shift occurs from 0.17 to 0.33.

The circular dichroism analysis in the far and near UV regions of the spectra in Figure 6A(1) and Figure 6 (1) turned out to provide some valuable information to the problem just discussed. The starting molar ellipticity of the H1-containing [3500 deg cm^2 (dmol)$^{-1}$] and H1-depleted [5900 deg cm^2 (dmol)$^{-1}$] fractions at 265 nm (Figure 6A) was very similar to the values reported earlier for equivalent samples.[44] The increase in the molecular ellipticity at 265 nm which can be taken as indicative of the DNA being freed from the histone interactions reaches a plateau at a concentration of approximately 0.5 mol of drug per mol of bp [Figure 6A(2)], as would

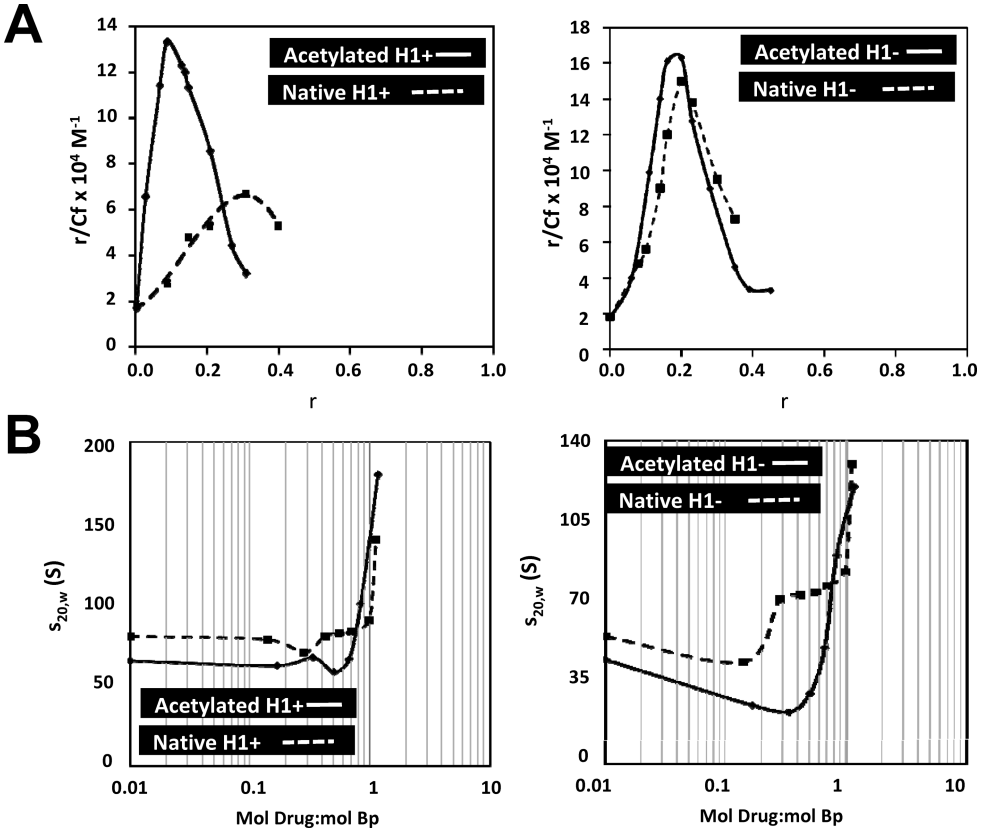

Figure 5. Characterization of the interaction of acetylated chromatin containing (H1+) or lacking (H1−) histone H1 with daunomycin: (A) Scatchard plot analysis of the binding of daunomycin; (B) dependence of the average sedimentation coefficient $s_{20,w}{}^{avg}$ as a function of the mol daunomycin/mol bp.

Table 2. Binding Constants of Daunomycin to Chromatin in the Presence (+H1) or upon Removal (−H1) of Histone H1

chromatin sample	binding constant (M^{-1})
acetylated, +H1[a]	4.9×10^4
acetylated, −H1[a]	6.8×10^4
native, +H1	4.6×10^4
native, −H1	6.4×10^4

[a] From ref 17.

Table 3. Analysis of Acetylated Chromatin Folding for the Samples Used in This Work in the Presence (+H1) or upon Removal (−H1) of Histone H1, As Determined by the Change in Sedimentation Coefficient ($s_{20,w}$) at Low (5 mM) and High (80 mM) Salt Concentration

chromatin sample	$s_{20,w}$ at 5 mM NaCl	$s_{20,w}$ at 80 mM NaCl
acetylated chromatin, +H1	65 S	93 S
acetylated chromatin, −H1	45 S	68 S

be predicted from full intercalation. It is interesting to note that the increase observed with the histone H1 depleted fraction is much higher in the sample lacking histone H1, and indeed, the molar ellipticity values reached at the plateau [13000−14000 deg cm^2 $(dmol)^{-1}$] are those that would be expected from a free DNA molecule.[45,46] In contrast, the values observed with the H1 containing fraction are much lower and the transition is less pronounced. This is in agreement with what was observed with the nucleosome counterparts when analyzed in the analytical ultracentrifuge (Figure 3C) that showed the presence of a large amount of free DNA at 0.669 mol drug/mol bp in the H1 depleted nucleosome when compared to the H1 containing particle.

The variation of the molar ellipticity in the visible range exhibits a more complex pattern. When the dependence of the ellipticity at 395 nm was plotted as a function of the drug/bp molar ratio for the acetylated fraction containing or lacking histone H1, a minimum was found at around 0.15−0.2 mol drug/mol bp [Figure 6B (2)]. If we consider that the average repeat length of chromatin is around 200 bp,[47] this implies that such decrease involves the intercalation of drug up to approximately 60 bp (considering that 0.5 mol drug/mol bp corresponds to 100% intercalation). The number of base pairs determined under this assumption corresponds to that of the average linker DNA length in chromatin [145 bp corresponding to the nucleosome core particle[47]]. Circular dichroism in the far UV region of the spectra contributed by the absorption of a DNA intercalating ligand such as daunomycin provides additional useful information about its intercalation mode.[48] A perpendicular angular orientation of the intercalator relative to the base pair dyad axis, such as that which is observed when daunomycin interacts with naked DNA,[40] yields a negative induced circular dichroism which changes to positive in a parallel orientation.[48] This suggests that binding of daunomycin to chromatin exhibits a complex pattern in which initial binding to the most accessible DNA regions of the linker proceeds as with naked DNA, resulting in a stiffening of the chromatin fiber that leads to a decrease in its sedimentation coefficient which is more noticeable in the H1-lacking complexes (Figure 5B) and alters the way in which the drug subsequently binds to DNA. The change in the orientation of the drug indicated by the transition from negative to positive ellipticity shown in Figure 6B(2) also provides support for the alterations of the linker twist associated with this chromatin unfolding process. As discussed in the previous section, this is further

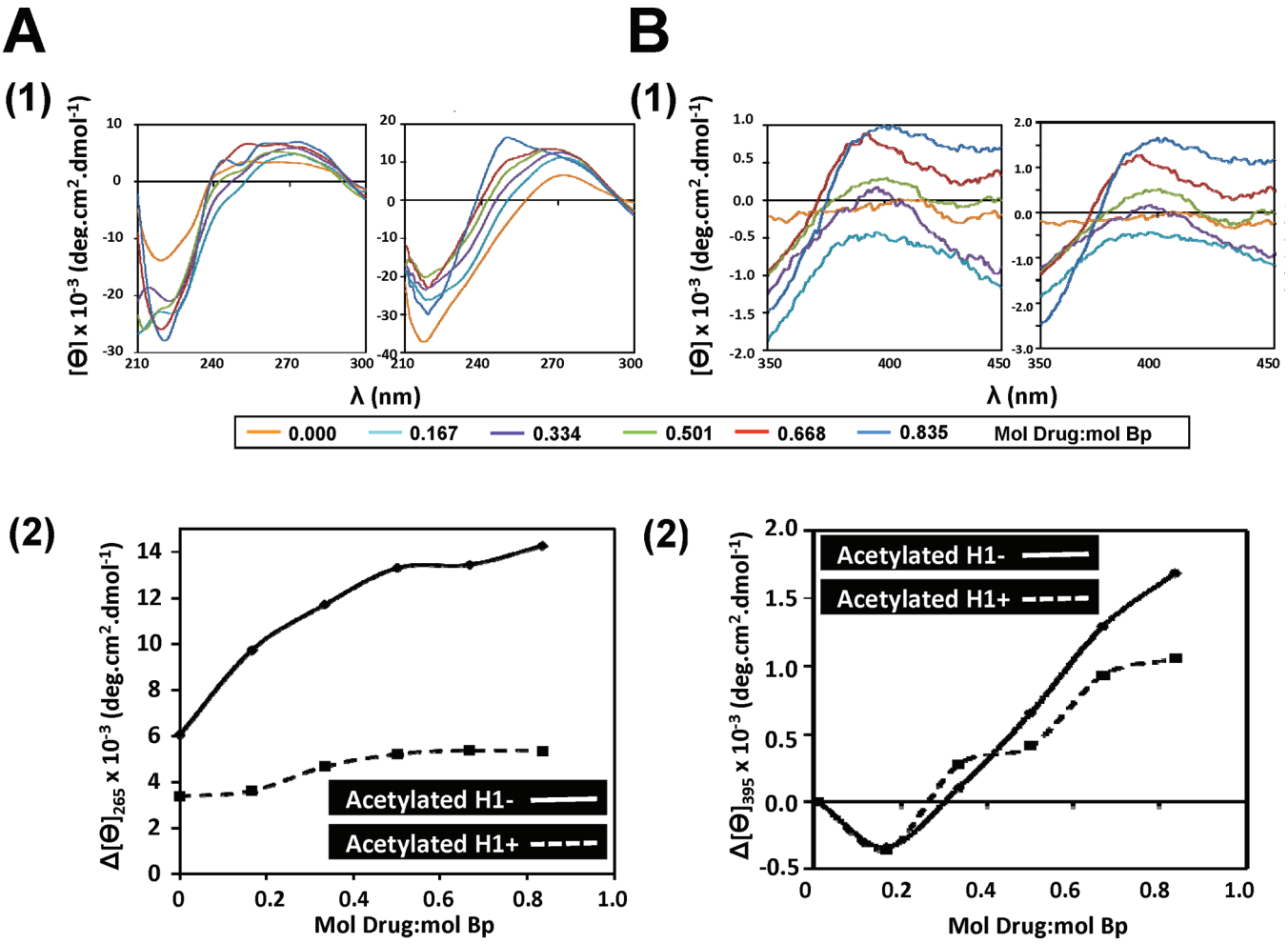

Figure 6. Circular dichroism analysis of the interaction of acetylated chromatin containing (H1+) or lacking (H1−) histone H1at different mol daunomycin:mol bp ratios: (A, B) (1) molar ellipticity as a function of wavelength; (A, B) (2) plot of the molar ellipticity at 265 nm as a function of mol daunomycin/mol bp.

accompanied by a disruption of the histone−DNA contacts and histone release that lead to chromatin aggregation.

Concluding Remarks. The structural effects resulting from the interaction of daunomycin with nucleosomes and chromatin are summarized in the model shown in Figure 7. The drug intercalation between base pairs starts at the flanking DNA regions of the nucleosome, unfolding the particle (9 S particle) and eventually leading to a full dissociation of the histones from DNA (5 S). The thicker arrow indicates that the dissociation process is facilitated by histone acetylation (Figure 3C). The partially unfolded particles, released histone H1, and fully dissociated DNA come together to produce aggregates with different size (sedimentation coefficients of >17 S). The size and complexity of the aggregates depend on the presence of histone H1 and core histone acetylation (Figure 4A). It increases with the presence of H1 and decreases with acetylation (as indicated by the arrows of different thickness) and by the schematic representation shown on the right-hand side of Figure 7A. In the case of the chromatin fiber, the intercalation of daunomycin in the linker DNA regions accessible to binding results in a change in the DNA twist that leads to unfolding (not shown) and aggregation.[13,17] The increase in the linker DNA accessible in the acetylated chromatin enhances the binding affinity of the drug (Figure 5A) and delays (depicted by the thinner arrow) the aggregation process (Figure 5B).

Despite the plethora of side effects derived from the chemotherapeutical use of anthracycline drugs in the treatment of many malignancies,[49] these drugs are still actively used in cancer therapies and new derivatives targeted to specific cancers are actively being developed and tested.[50] Although daunomycin derivatives may have multifaceted downstream molecular effects,[12] one of their main roles stems from their ability to bind to chromatin and interfere with gene expression.[27] Treatment of yeast cells with concentrations that do not interfere with their viability has allowed the identification of genes targeted by the drug in this organism.[51] Furthermore, analyses of the effects of daunorubicin on the yeast transcriptome have demonstrated that the drug interferes with transcription factor binding through binding competition with their target sequences.[52] One does not need to invoke the high drug/bp ratios used in this work. Indeed it is evident that even at the lowest ratios used by us and below, intercalation takes place with high affinity leading to changes in the DNA twist which in the context of the cell will immediately lead to changes in DNA supercoiling. Intercalation of daunomycin into DNA distorts the DNA double helix,[40] an effect that with supercoiled DNA and nucleosomes takes place at very low drug concentrations.[14] Both DNA supercoiling and histone acetylation have long been shown to play a role in chromatin activation in preparation for gene expression.[53]

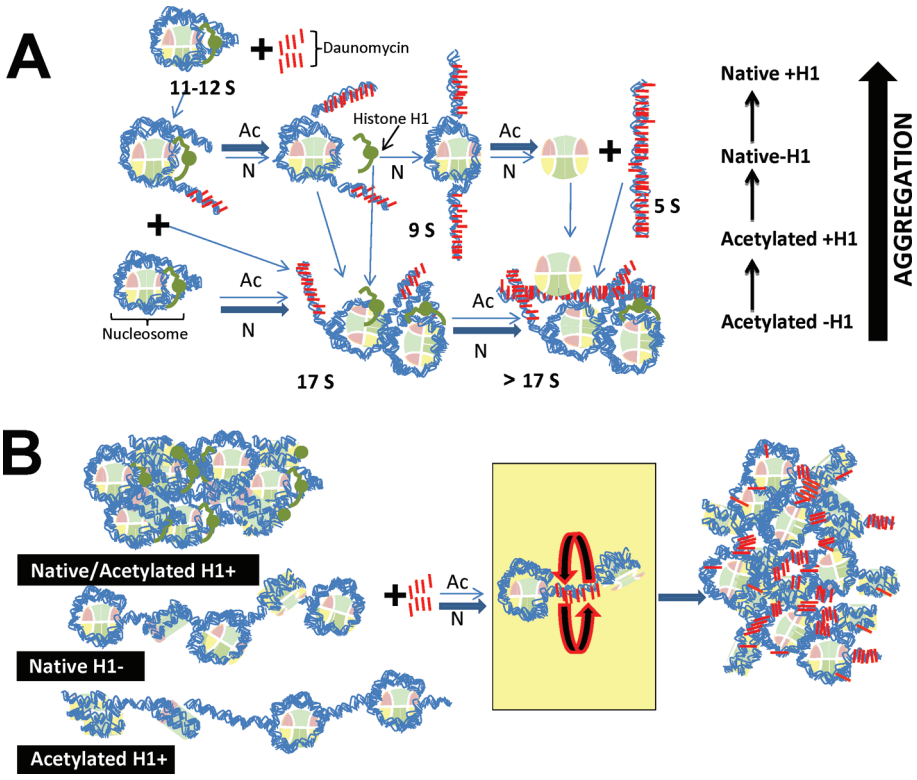

Figure 7. Models to explain the effects resulting from the interaction of daunomycin with nucleosomes (A) and with chromatin (B).

The work described here is of particular importance at a time when daunomycin starts being used in combination with HDAC inhibitors as well as hormone antagonists such as tamoxifen with potential for regulation of gene expression to treat a variety of cancers such as acute myeloid and refractory leukemias[54,55] and breast cancer.[56,57] Valproic acid and 3-(dimethylaminomethyl)-*N*-[2-[4-(hydroxycarbamoyl)phenoxy]ethyl]-1-benzofuran-2-carboxamide (PCI-24781 HDAC inhibitor) have been recently shown to potentiate the therapeutic effects of anthracyclines[58] and to sensitize human and canine osteosarcomas leading to decreased proliferation and increased apoptosis.[59]

In addition to all this, this work sheds some additional light on the structural transitions affecting chromatin as a result of histone acetylation. Comparison of Figure 4A and Figure 5B shows that while the starting point of daunomycin-dependent aggregation of nucleosomes occurs at nearly the same mol drug/mol bp ratios (Figure 4A), in the case of the oligonucleosome fractions the starting point occurs at higher ratios (Figure 5B), an effect that is even more noticeable in the histone H1-depleted fractions. This observation is consistent with the role of histone acetylation in releasing the linker DNA regions flanking the nucleosome to open chromatin structure.[24,25]

Acknowledgment. This work was supported by Canadian Institute of Health Research (CIHR) Grant MOP-97878 to J.A. and by a Natural Sciences and Engineering Research Council (NSERC) Discovery Grant 138216-09 to F.Y.M.C. L.S. was the recipient of a British Columbia Cancer Studentship.

References

(1) Lown, J. W. Discovery and development of anthracycline antitumour antibiotics. *Chem. Soc. Rev.* **1993**, *22*, 165–176.
(2) Di Marco, A.; Gaetani, M.; Scarpinato, B. Adriamycin (NSC-123,127): a new antibiotic with antitumour activity. *Cancer Chemother. Rep.* **1969**, *53*, 33–37.
(3) Buchner, T.; Berdel, W. E.; Hiddemann, W. Priming with granulocyte colony-stimulating factor—relation to high-dose cytarabine in acute myeloid leukemia. *N. Engl. J. Med.* **2004**, *350*, 2215–2216.
(4) Carrion, C.; de Madariaga, M. A.; Domingo, J. C. In vitro cytotoxic study of immunoliposomal doxorubicin targeted to human CD34(+) leukemic cells. *Life Sci.* **2004**, *75*, 313–328.
(5) Andre, F.; Delaloge, S. First-generation genomic tests for breast cancer treatment. *Lancet Oncol.* **2010**, *11*, 6–7.
(6) Gigli, M.; Doglia, S. M.; Millot, J. M.; Valentini, L.; Manfait, M. Quantitative study of doxorubicin in living cell nuclei by microspectrofluorometry. *Biochim. Biophys. Acta* **1988**, *950*, 13–20.
(7) Belloc, F.; Lacombe, F.; Dumain, P.; Lopez, F.; Bernard, P.; Boisseau, M. R.; Reifers, J. Intercalation of anthracyclines into living cell DNA analyzed by flow cytometry. *Cytometry* **1992**, *13*, 880–885.
(8) Davies, C. L.; Duffy, P. M.; MacRobert, A. J.; Loizidou, M. C.; Cooper, A. J.; Taylor, I. Localization of anthracycline accumulation in sensitive and resistant urothelial tumor cell lines. *Cancer Detect. Prev.* **1996**, *20*, 625–633.
(9) Frederick, C. A.; Williams, L. D.; Ughetto, G.; van der Marel, G. A.; van Boom, J. H.; Rich, A.; Wang, A. H. Structural comparison of anticancer drug−DNA complexes: adriamycin and daunomycin. *Biochemistry* **1990**, *29*, 2538–2549.
(10) Quigley, G. J.; Wang, A. H.; Ughetto, G.; van der Marel, G.; van Boom, J. H.; Rich, A. Molecular structure of an anticancer drug−DNA complex: daunomycin plus d(CpGpTpApCpG). *Proc. Natl. Acad. Sci. U.S.A.* **1980**, *77*, 7204–7208.
(11) Roche, C. J.; Berkowitz, D.; Sulikowski, G. A.; Danishefsky, S. J.; Crothers, D. M. Binding affinity and site selectivity of daunomycin analogues. *Biochemistry* **1994**, *33*, 936–942.
(12) Rabbani, A.; Finn, R. M.; Ausio, J. The anthracycline antibiotics: antitumor drugs that alter chromatin structure. *BioEssays* **2005**, *27*, 50–56.
(13) Fritzsche, H.; Wahnert, U.; Chaires, J. B.; Dattagupta, N.; Schlessinger, F. B.; Crothers, D. M. Anthracycline antibiotics. Interaction with DNA and nucleosomes and inhibition of DNA synthesis. *Biochemistry* **1987**, *26*, 1996–2000.
(14) Simpkins, H.; Pearlman, L. F.; Thompson, L. M. Effects of adriamycin on supercoiled DNA and calf thymus nucleosomes studied with fluorescent probes. *Cancer Res.* **1984**, *44*, 613–618.
(15) Patel, D. J.; Kozlowski, S. A.; Rice, J. A. Hydrogen bonding, overlap geometry, and sequence specificity in anthracycline antitumor

antibiotic.DNA complexes in solution. *Proc. Natl. Acad. Sci. U.S.A.* **1981**, *78*, 3333–3337.
(16) Chaires, J. B.; Dattagupta, N.; Crothers, D. M. Binding of daunomycin to calf thymus nucleosomes. *Biochemistry* **1983**, *22*, 284–292.
(17) Rabbani, A.; Iskandar, M.; Ausió, J. Daunomycin-induced unfolding and aggregation of chromatin. *J. Biol. Chem.* **1999**, *274*, 18401–18406.
(18) Calestagne-Morelli, A.; Ausio, J. Long-range histone acetylation: biological significance, structural implications, and mechanisms. *Biochem. Cell Biol.* **2006**, *84*, 518–527.
(19) Ausió, J.; van Holde, K. E. Histone hyperacetylation: its effects on nucleosome conformation and stability. *Biochemistry* **1986**, *25*, 1421–1428.
(20) Bauer, W. R.; Hayes, J. J.; White, J. H.; Wolffe, A. P. Nucleosome structural changes due to acetylation. *J. Mol. Biol.* **1994**, *236*, 685–690.
(21) Oliva, R.; Bazett-Jones, D. P.; Locklear, L.; Dixon, G. H. Histone hyperacetylation can induce unfolding of the nucleosome core particle. *Nucleic Acids Res.* **1990**, *18*, 2739–2747.
(22) Dunker, A. K.; Lawson, J. D.; Brown, C. J.; Williams, R. M.; Romero, P.; Oh, J. S.; Oldfield, C. J.; Campen, A. M.; Ratliff, C. M.; Hipps, K. W.; Ausió, J.; Nissen, M. S.; Reeves, R.; Kang, C.; Kissinger, C. R.; Bailey, R. W.; Griswold, M. D.; Chiu, W.; Garner, E. C.; Obradovic, Z. Intrinsically disordered protein. *J. Mol. Graphics Modell.* **2001**, *19*, 26–59.
(23) Wang, X.; He, C.; Moore, S. C.; Ausió, J. Effects of histone acetylation on the solubility and folding of the chromatin fiber. *J. Biol. Chem.* **2001**, *276*, 12764–12768.
(24) Norton, V. G.; Imai, B. S.; Yau, P.; Bradbury, E. M. Histone acetylation reduces nucleosome core particle linking number change. *Cell* **1989**, *57*, 449–457.
(25) Garcia Ramirez, M.; Rocchini, C.; Ausió, J. Modulation of chromatin folding by histone acetylation. *J. Biol. Chem.* **1995**, *270*, 17923–17928.
(26) Studzian, K.; Wasowska, M.; Piestrzeniewicz, M. K.; Wilmanska, D.; Szmigiero, L.; Oszczapowicz, I.; Gniazdowski, M. Inhibition of RNA synthesis in vitro and cell growth by anthracycline antibiotics. *Neoplasma* **2001**, *48*, 412–418.
(27) Ito, H.; Murakami, M.; Furuhata, A.; Gao, S.; Yoshida, K.; Sobue, S.; Hagiwara, K.; Takagi, A.; Kojima, T.; Suzuki, M.; Banno, Y.; Tanaka, K.; Tamiya-Koizumi, K.; Kyogashima, M.; Nozawa, Y.; Murate, T. Transcriptional regulation of neutral sphingomyelinase 2 gene expression of a human breast cancer cell line, MCF-7, induced by the anti-cancer drug, daunorubicin. *Biochim. Biophys. Acta* **2009**, *1789*, 681–690.
(28) Phillips, D. M. The presence of acetyl groups of histones. *Biochem. J.* **1963**, *87*, 258–263.
(29) Allfrey, V. G.; Faulkner, R.; Mirsky, A. E. Acetylation and methylation of histones and their possible role in the regulation of rna synthesis. *Proc. Natl. Acad. Sci. U.S.A.* **1964**, *51*, 786–794.
(30) Mizzen, C. A.; Allis, C. D. Linking histone acetylation to transcriptional regulation. *Cell. Mol. Life Sci.* **1998**, *54*, 6–20.
(31) Wang, X.; Moore, S. C.; Laszckzak, M.; Ausió, J. Acetylation increases the alpha-helical content of the histone tails of the nucleosome. *J. Biol. Chem.* **2000**, *275*, 35013–35020.
(32) Libertini, L. J.; Small, E. W. Salt induced transitions of chromatin core particles studied by tyrosine fluorescence anisotropy. *Nucleic Acids Res.* **1980**, *8*, 3517–3534.
(33) Laemmli, U. K. Cleavage of structural proteins during the assembly of the head of bacteriophage T4. *Nature* **1970**, *227*, 680–685.
(34) Shaw, B. R.; Cognetti, G.; Sholes, W. M.; Richards, R. G. Shift in nucleosome populations during embryogenesis: microheterogeneity in nucleosomes during development of the sea urchin embryo. *Biochemistry* **1981**, *20*, 4971–4978.
(35) Yager, T. D.; van Holde, K. E. Dynamics and equilibria of nucleosomes at elevated ionic strength. *J. Biol. Chem.* **1984**, *259*, 4212–4222.
(36) Scatchard, G. The attractions of proteins for small molecules and ions. *Ann. N.Y. Acad. Sci.* **1949**, *51*, 660–672.
(37) Demeler, B.; Brookes, E.; Nagel-Steger, L. Analysis of heterogeneity in molecular weight and shape by analytical ultracentrifugation using parallel distributed computing. *Methods Enzymol.* **2009**, *454*, 87–113.
(38) Read, C. M.; Baldwin, J. P.; Crane-Robinson, C. Structure of subnucleosomal particles. Tetrameric (H3/H4)2 146 base pair DNA and hexameric (H3/H4)2(H2A/H2B)1 146 base pair DNA complexes. *Biochemistry* **1985**, *24*, 4435–4450.
(39) Luger, K.; Mader, A. W.; Richmond, R. K.; Sargent, D. F.; Richmond, T. J. Crystal structure of the nucleosome core particle at 2.8 Å resolution. *Nature* **1997**, *389*, 251–260.
(40) Wang, A. H.; Ughetto, G.; Quigley, G. J.; Rich, A. Interactions between an anthracycline antibiotic and DNA: molecular structure of daunomycin complexed to d(CpGpTpApCpG) at 1.2-Å resolution. *Biochemistry* **1987**, *26*, 1152–1163.
(41) Tatchell, K.; van Holde, K. E. Reconstitution of chromatin core particles. *Biochemistry* **1977**, *16*, 5295–5303.
(42) McMurray, C. T.; van Holde, K. E. Binding of ethidium bromide causes dissociation of the nucleosome core particle. *Proc. Natl. Acad. Sci. U.S.A.* **1986**, *83*, 8472–8476.
(43) Ausió, J.; Borochov, N.; Seger, D.; Eisenberg, H. Interaction of chromatin with NaCl and $MgCl_2$. Solubility and binding studies, transition to and characterization of the higher-order structure. *J. Mol. Biol.* **1984**, *177*, 373–398.
(44) Reczek, P. R.; Weissman, D.; Huvos, P. E.; Fasman, G. D. Sodium butyrate induced structural changes in HeLa cell chromatin. *Biochemistry* **1982**, *21*, 993–1002.
(45) Cowman, M. K.; Fasman, G. D. Circular dichroism analysis of mononucleosome DNA conformation. *Proc. Natl. Acad. Sci. U.S.A.* **1978**, *75*, 4759–4763.
(46) Fasman, G. D. Circular dichroism analysis of chromatin and DNA−nuclear protein complexes. *Methods Cell Biol.* **1978**, *18*, 327–349.
(47) van Holde, K. E. *Chromatin*: Springer-Verlag: New York, 1988.
(48) Lyng, R.; Hard, T.; Norden, B. Induced CD of DNA intercalators: electric dipole allowed transitions. *Biopolymers* **1987**, *26*, 1327–1345.
(49) Carvalho, C.; Santos, R. X.; Cardoso, S.; Correia, S.; Oliveira, P. J.; Santos, M. S.; Moreira, P. I. Doxorubicin: the good, the bad and the ugly effect. *Curr. Med. Chem.* **2009**, *16*, 3267–3285.
(50) Park, H. J.; Chung, H. J.; Min, H. Y.; Park, E. J.; Hong, J. Y.; Kim, W. B.; Kim, S. H.; Lee, S. K. Inhibitory effect of DA-125, a new anthracyclin analog antitumor agent, on the invasion of human fibrosarcoma cells by down-regulating the matrix metalloproteinases. *Biochem. Pharmacol.* **2005**, *71*, 21–31.
(51) Xia, L.; Jaafar, L.; Cashikar, A.; Flores-Rozas, H. Identification of genes required for protection from doxorubicin by a genome-wide screen in *Saccharomyces cerevisiae*. *Cancer Res.* **2007**, *67*, 11411–11418.
(52) Rojas, M.; Casado, M.; Portugal, J.; Pina, B. Selective inhibition of yeast regulons by daunorubicin: a transcriptome-wide analysis. *BMC Genomics* **2008**, *9*, 358.
(53) Gross, D. S.; Garrard, W. T. Poising chromatin for transcription. *Trends Biochem. Sci.* **1987**, *12*, 293–297.
(54) Kadia, T. M.; Yang, H.; Ferrajoli, A.; Maddipotti, S.; Schroeder, C.; Madden, T. L.; Holleran, J. L.; Egorin, M. J.; Ravandi, F.; Thomas, D. A.; Newsome, W.; Sanchez-Gonzalez, B.; Zwiebel, J. A.; Espinoza-Delgado, I.; Kantarjian, H. M.; Garcia-Manero, G. A phase I study of vorinostat in combination with idarubicin in relapsed or refractory leukaemia. *Br. J. Haematol.* **2010**, *150*, 72–82.
(55) Fathi, A. T.; Grant, S.; Karp, J. E. Exploiting cellular pathways to develop new treatment strategies for AML. *Cancer Treat. Rev.* **2010**, *36*, 142–150.
(56) Albain, K. S.; Barlow, W. E.; Ravdin, P. M.; Farrar, W. B.; Burton, G. V.; Ketchel, S. J.; Cobau, C. D.; Levine, E. G.; Ingle, J. N.; Pritchard, K. I.; Lichter, A. S.; Schneider, D. J.; Abeloff, M. D.; Henderson, I. C.; Muss, H. B.; Green, S. J.; Lew, D.; Livingston, R. B.; Martino, S.; Osborne, C. K. Adjuvant chemotherapy and timing of tamoxifen in postmenopausal patients with endocrine-responsive, node-positive breast cancer: a phase 3, open-label, randomised controlled trial. *Lancet* **2009**, *374*, 2055–2063.
(57) Albain, K. S.; Barlow, W. E.; Shak, S.; Hortobagyi, G. N.; Livingston, R. B.; Yeh, I. T.; Ravdin, P.; Bugarini, R.; Baehner, F. L.; Davidson, N. E.; Sledge, G. W.; Winer, E. P.; Hudis, C.; Ingle, J. N.; Perez, E. A.; Pritchard, K. I.; Shepherd, L.; Gralow, J. R.; Yoshizawa, C.; Allred, D. C.; Osborne, C. K.; Hayes, D. F. Prognostic and predictive value of the 21-gene recurrence score assay in postmenopausal women with node-positive, oestrogen-receptor-positive breast cancer on chemotherapy: a retrospective analysis of a randomised trial. *Lancet Oncol.* **2010**, *11*, 55–65.
(58) Yang, C.; Choy, E.; Hornicek, F. J.; Wood, K. B.; Schwab, J. H.; Liu, X.; Mankin, H.; Duan, Z. Histone deacetylase inhibitor (HDACI) PCI-24781 potentiates cytotoxic effects of doxorubicin in bone sarcoma cells. *Cancer Chemother. Pharmacol.* [Online early access]. DOI: 10.1007/s00280-010-1344-7. Published Online: May 12, 2010.
(59) Wittenburg, L. A.; Bisson, L.; Rose, B. J.; Korch, C.; Thamm, D. H. The histone deacetylase inhibitor valproic acid sensitizes human and canine osteosarcoma to doxorubicin. *Cancer Chemother. Pharmacol.* [Online early access]. DOI: 10.1007/s00280-010-1287-z. Published Online: March 20, 2010.